# Gamma Decay of the 3.90-MeV ($2^+$) Level in $Ca^{40}$†

Jack R. MacDonald
*Bell Telephone Laboratories, Murray Hill, New Jersey 07971, Rutgers University, New Brunswick, New Jersey 07102, and Brookhaven National Laboratory, Upton, New York 11973*

and

D. H. Wilkinson
*Brookhaven National Laboratory, Upton, New York 11973, and Nuclear Physics Laboratory, Oxford, England*

and

D. E. Alburger
*Brookhaven National Laboratory, Upton, New York 11973*

(Received 18 September 1970)

The lifetime and $\gamma$-ray branching of the 3.90-MeV ($2^+$) state of $Ca^{40}$ have been measured using the reactions $Ca^{40}(p,p')Ca^{40*}$ at a bombarding energy of 7.32 MeV and $K^{39}(p,\gamma)Ca^{40}$ at the $E_p = 1.344$-MeV resonance. Consistent values for the lifetime were obtained from the Doppler shifts of the 3.90-MeV $\gamma$ rays in both reactions and from the 0° line shape in the $K^{39}(p,\gamma)Ca^{40}$ reaction. A value of $\tau = 50 \pm 5$ fsec is adopted for the mean lifetime of the 3.90-MeV state. The 3.90 → 3.35-MeV branching ratio was measured by observing the 0.555-MeV cascade $\gamma$ rays in quadruple coincidence with the two annihilation $\gamma$ rays and the inelastic protons in the $Ca^{40}(p,p')Ca^{40*}$ reaction, or in triple coincidence with annihilation $\gamma$ rays in the $K^{39}(p,\gamma)Ca^{40}$ reaction. Results are in agreement and the adopted branch is $(7.95 \pm 0.8) \times 10^{-4}$. By combining the lifetime and branching results, the 0.555-MeV $E2$ transition rate corresponds to a $B(E2;\ 3.90\ (2^+) \rightarrow 3.35\ (0^+))$ of $250 \pm 35\ e^2\ \text{fm}^4$. This result is in excellent agreement with recent theoretical estimates of the transition strength. The mean lifetime of the 5.28-MeV ($4^+$) state of $Ca^{40}$ was measured to be $310 \pm 60$ fsec. The corresponding $B(E2;\ 5.28\ (4^+) \rightarrow 3.90\ (2^+1))$ of $535 \pm 110\ e^2\ \text{fm}^4$ is in reasonable agreement with expectations based on a strong-deformation rotational model of the states.

## I. INTRODUCTION

The positive-parity levels of $Ca^{40}$ below 7-MeV excitation energy (see Fig. 1) exhibit many properties characteristic of collective structure. Recent measurements of spins, parities, and transition probabilities[1-10] suggest the existence of three rotational-type bands. This classification of levels can be adequately, if not uniquely, understood in terms of the nuclear model of Gerace and Green[11,12] who describe these states as mixtures of spherical-shell-model and multiparticle, multihole deformed states. In particular, states at 3.35-MeV ($0^+$), 3.90-MeV ($2^+$), and 5.28-MeV ($4^+$) are described as strongly deformed states whose major configuration involves the promotion of four particles from the *sd* to the *fp* shell. The energy spacing of these states and the large in-band $E2$ strength of the $4^+ \rightarrow 2^+$ transition are consistent with such a strong-deformation description. For such a strong-deformation rotational model, the strength of the in-band $2^+ \rightarrow 0^+$ transition is closely related to that of the $4^+ \rightarrow 2^+$ transition; it would be very difficult to understand a strength for the former transition that departed greatly from the expectation of the model unless the rotational picture were in fact invalid and the level spacings coincidental. It is, therefore, important as a confirmation even of the qualitative correctness of the rotational picture to establish that the strength of the $2^+ \rightarrow 0^+$ transition in question is large and is correctly related to that of the $4^+ \rightarrow 2^+$ transition. This is the origin of our interest in this matter.

The determination of the strength of the in-band $2^+ \rightarrow 0^+$ transition demands knowledge of the lifetime of the $2^+$ state and its relative decay to the ground and first excited $0^+$ states. Measurements of the lifetime of this level by Doppler-shift,[5-8,13] inelastic electron scattering,[14,15] and resonance-fluorescence[16,17] techniques yield conflicting results (Table I). Furthermore, a preliminary measurement[18] of the cascade-to-crossover branching ratio of the 3.90-MeV ($2^+$) state resulted in an in-band transition strength which was totally inconsistent with the theory of Gerace and Green[11,12] and with the later experimental result of Canada *et al.*[19] It was the purpose of the present work to measure the branching ratio and lifetime of the

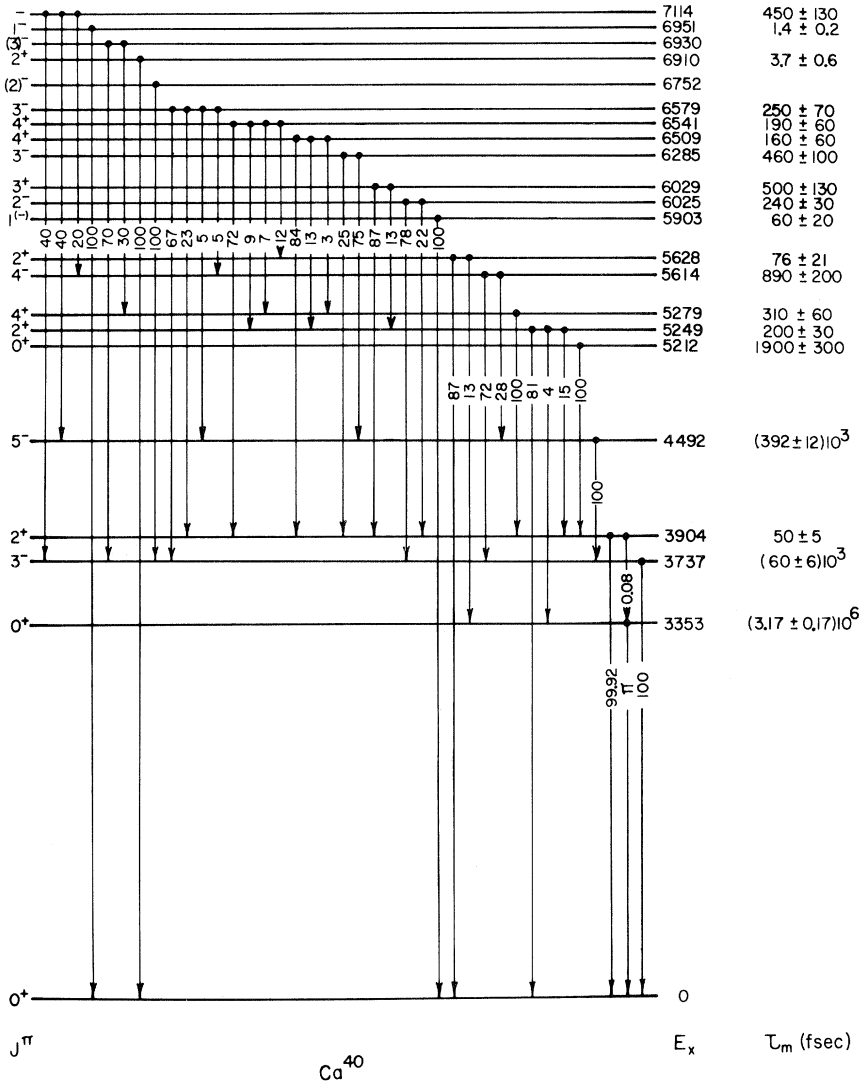


FIG. 1. Energy levels of $Ca^{40}$. Spins, parities, excitation energies, mean lifetimes, and decay schemes have been taken from Refs. 1–10 and references contained therein.

3.90-MeV ($2^+$) state utilizing the $Ca^{40}(p,p'\gamma)Ca^{40}$ and $K^{39}(p,\gamma)Ca^{40}$ reactions in each case in an attempt to resolve the experimental discrepancies.

## II. EXPERIMENTAL METHODS

### A. Lifetime Measurements

#### 1. $(p,p'\gamma)$ Reaction

The lifetime of the 3.90-MeV ($2^+$) state was measured utilizing a Doppler-shift-attenuation technique which has been described in detail by MacDonald *et al.*[5] and by Bertin *et al.*[20] The state was excited via the $(p,p')$ reaction utilizing the Rutgers-Bell tandem accelerator at a bombarding energy of 7.32 MeV, at which energy the backscattered yield from the level of interest is particularly high. A self-supporting natural calcium target of thickness 2 mg/cm$^2$ was used for the measurements. Protons scattered to angles between 168 and 172° were detected in an annular surface-barrier detector; decay $\gamma$ rays in coincidence with backscattered particles were detected in a 30-cm$^3$ Ge(Li) detector placed alternately at forward and backward angles with respect to the incident-beam direction. As a further check on the method, the lifetime of the 5.28-MeV ($4^+$) state was measured using protons of energy 9.31 MeV for comparison with previous results.

#### 2. $K^{39}(p,\gamma)$ Reaction

The 3.90-MeV level in $Ca^{40}$ was populated via the reaction $K^{39}(p,\gamma)$ at a bombarding energy of

1.344 MeV using a proton beam from the 3.5-MV Van de Graaff accelerator at Brookhaven. The decay of the 9.646-MeV state in $Ca^{40}$ formed at this resonance has been studied by Leenhouts and Endt[2] and by Lindeman *et al.*[8] According to the more recent measurements by the latter, the resonance state decays with $\gamma$-ray branches of 47% to the 3.90-MeV state, 42% to the $3^-$ level at 3.74 MeV, and the remaining 11% to states at 5.63 and 7.47 MeV, both of which decay predominantly to the ground state. The lifetime of the 3.90-MeV state was determined by measuring the 90°-0° Doppler shift of the ground-state $\gamma$-ray transition, as well as from an analysis of the line shape of the $\gamma$-ray peak at 0°. The target consisted of $K_2SO_4$ enriched to 99.97% in $K^{39}$, evaporated in a layer approximately 50 $\mu g/cm^2$ thick onto 0.005-in.-thick gold. A 3-cm-diam disk of the gold-backed target was clamped onto the end of a target chamber at an angle of 45° to the incident beam. The gold disk, which formed the vacuum seal, was cooled by an atomizer water spray which permitted a 15–20-$\mu$A beam to be used with no apparent target deterioration during long bombardment times. $\gamma$ rays were detected in a 20-$cm^3$ Ge(Li) detector which had 3.7-keV resolution for the 2.614-MeV $\gamma$ rays of a ThC″ source which served to monitor gain changes during the runs.

### B. Branching-Ratio Measurements

A branch of the 3.90-MeV ($2^+$) level to the 3.35-MeV ($0^+$) level would be characterized by a 0.555-MeV $\gamma$ ray in coincidence with the electron and positron from the pair decay of the $0^+$ state. By insuring that the positron annihilates in the immediate vicinity of the target, the transition would result in a triple coincidence of a 0.555-MeV $\gamma$ ray with two oppositely directed 0.511-MeV annihilation quanta. This identifying signature formed the basis of both the $(p,p'\gamma)$ and $(p,\gamma)$ branching-ratio measurements.

In both experiments, four 3-in. by 3-in. NaI(Tl) crystals were placed at 90° intervals around, and 5 cm from, the target in the plane passing through the target perpendicular to the beam axis. The detectors were selected for the similarity of their performance and had energy resolutions for 0.662-MeV $\gamma$ rays in the range 7.6 to 8.1%. The gains of the detectors were set equal and then stabilized using Spectrostat gain-stabilization units operating on the 0.854-MeV $\gamma$ rays of a $Mn^{54}$ source.

#### 1. $(p,p'\gamma)$ Measurement

In this measurement, the 3.90-MeV state was excited by inelastic proton scattering as in the lifetime measurement. The target, consisting of 500-$\mu g/cm^2$ natural calcium evaporated onto a 10-$\mu g/cm^2$ carbon foil, was placed in a 1.5-cm-diam by 2-cm-long aluminum cylinder which had suitable entrance and exit holes for the beam and was positioned symmetrically on the beam axis. Particles backscattered near 180° were detected in an annular surface-barrier detector. Approximately 30% of the total proton count rate corresponded to excitation of the level of interest, typically 2000 excitations per sec. The aluminum cylinder was sufficiently thick to stop the positrons from the decay of the $0^+$ state; losses of positrons through exit and entrance channels amounted to approximately 16%.

A fast-slow coincidence system was used to select acceptable events in the following manner. A fast coincidence was required between events in the particle detector and any three (but not four) cyclically ordered NaI(Tl) detectors. In addition,

TABLE I. Summary of measurements of the mean lifetime of the 3.90-MeV ($2^+$) state of $Ca^{40}$.

| Experimental technique | Mean lifetime (fsec) |
|---|---|
| Inelastic electron scattering [a] | 31 ± 10 |
| Inelastic electron scattering [b] | 54 ± 7 |
| Resonance-fluorescence [c] | >47 |
| Resonance-fluorescence [d] | 45 ± 5 |
| Doppler-shift attenuation, $K^{39}(p,\gamma)Ca^{40}$ [e] | 19 ± 6 |
| Doppler-shift attenuation, $K^{39}(p,\gamma)Ca^{40}$ [f] | 25 ± 6 |
| Doppler-shift attenuation, $K^{39}(p,\gamma)Ca^{40}$ [g] | 58 ± 10 |
| Doppler-shift attenuation, $Ca^{40}(p,p'\gamma)Ca^{40}$ [h] | 64 ± 19 |
| Doppler-shift attenuation, $Ca^{40}(p,p'\gamma)Ca^{40}$ [i] | 54 ± 14 |
| Doppler-shift attenuation, $Ca^{40}(p,p'\gamma)Ca^{40}$ [j] | 48 ± 10 |
| Adopted value | 50 ± 5 |

[a] See Ref. 14.
[b] See Ref. 15.
[c] See Ref. 16.
[d] See Ref. 17.
[e] See Ref. 7.
[f] See Ref. 8.
[g] Present work
[h] See Ref. 5.
[i] See Ref. 13.
[j] Present work.

slow-coincidence energy conditions were imposed such that the particle energy corresponded to excitation of the 3.90-MeV level and the scintillator signals were consistent with photopeak detection of 0.511- or 0.555-MeV $\gamma$ rays. With the fourfold coincidence conditions satisfied, the analog signal from the middle NaI(Tl) crystal (which presumably detected a 0.555-MeV $\gamma$ ray) was gated into a pulse-height analyzer and routed into an appropriate section of memory for storage. Four such independent spectra (corresponding to the four $\gamma$-ray counters) were accumulated during a total running time of 25 h. The efficiency of the apparatus for detecting positrons was determined by measuring the count rate of triple coincidences between particles exciting the 3.35-MeV ($0^+$) state and the two annihilation quanta from the pair decay of the state. The measured pair detection efficiency of (2.71 $\pm$0.11)% for either pair of opposite crystals agreed well with that obtained using a $Na^{22}$ source placed in the target position.

### 2. $(p,\gamma)$ Measurement

The 3.90-MeV ($2^+$) level was populated as in the lifetime measurement using a similar target. The target chamber and detector geometry is illustrated in Fig. 2. The gold-backed target was soldered to the bottom of an aluminum target chamber having walls 0.4 cm thick, sufficient to stop the positrons from the pair decay of the 3.35-MeV ($0^+$) state, yet as thin as possible to reduce the background from high-energy $\gamma$ rays interacting via external pair production in the region of the target. A liquid-nitrogen cold trap served to reduce carbon buildup on the target. For water cooling of the target, a length of thin-walled aluminum tubing (not indicated in Fig. 2) was soldered to the outer end of the target chamber.

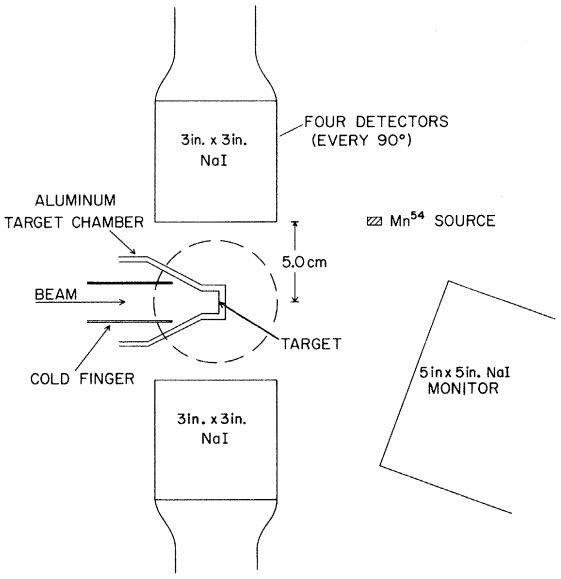


FIG. 2. Experimental arrangement for the branching-ratio measurement using the reaction $K^{39}(p,\gamma)Ca^{40}$.

The $\gamma$-ray detector geometry was similar to that used in the $(p,p'\gamma)$ experiment with the addition of a 5-in.-diam by 5-in.-long NaI(Tl) detector placed at 30° to the beam at a distance of 13.2 cm from the target in order to monitor the reaction yield of $\gamma$ rays and hence the total number of excitations of the 3.90-MeV level. Coincidence circuitry demanded fast-slow coincidences between three $\gamma$-ray detectors with energy conditions consistent with the detection of annihilation quanta by diametrically opposite crystals. The fourth counter was run in anticoincidence. This anticoincidence condition served to reduce unwanted 0.511-MeV background due to those events in which both high-energy $\gamma$ rays from the cascade decay of the 9.646-MeV resonance state (either 9.646 → 3.90 → 0 or 9.646 → 3.74 → 0) interacted via pair production in the vicinity of the target. Three of the four 0.511-MeV $\gamma$ rays so produced could satisfy the coincidence conditions in three crystals and result in a 0.511-MeV peak in the triple-coincidence spectrum. The fourth 0.511-MeV $\gamma$ ray would then have a high probability of interacting in the fourth crystal; in

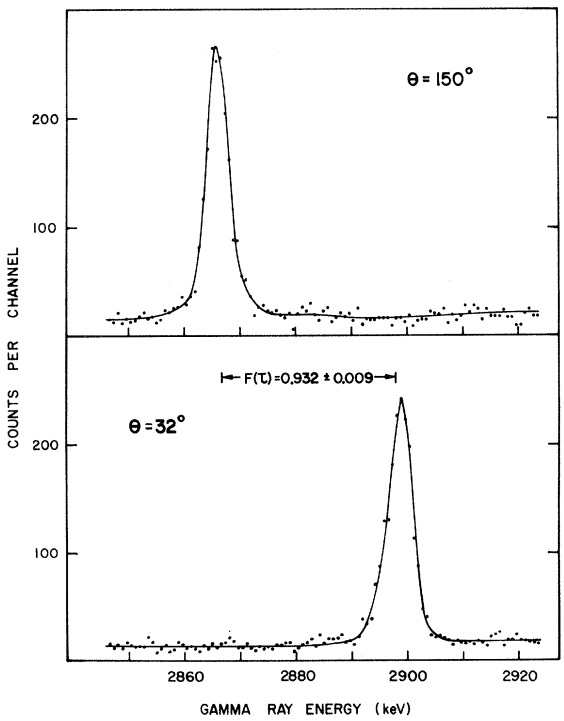


FIG. 3. Typical $p'$-$\gamma$ coincidence spectra indicating the Doppler shift of the "double-escape" peak of the 3.90-MeV $\gamma$ ray at forward and backward angles of observation. The $F(\tau)$ value indicated on the figure is that derived from the analysis of several such spectra.

fact, the anticoincidence condition reduced the undesirable peak by a factor of 2.7. As in the $(p,p'\gamma)$ experiment, the analog signal from the middle crystal was appropriately gated and routed into analyzer memory for storage.

The efficiency of the system for the detection of a positron annihilating in the target chamber was determined by placing a $Na^{22}$ source in the target position and measuring the intensity of the 1.275-MeV $\gamma$ ray in one of the detectors in singles and then in triple coincidence with annihilation radiation in the corresponding side crystals. After corrections for the known electron-capture decay, for analyzer dead time, for peak summing, and for $\gamma$-ray absorption in the source container, an efficiency of $(2.9\pm0.3)\%$ was measured for either pair of opposite NaI(Tl) detectors. A further check on the positron-detection efficiency was carried out by populating the 9.877-MeV level in $Ca^{40}$ at the 1.575-MeV resonance in the reaction $K^{39}(p,\gamma)$. This level has a 12% decay branch to the 3.35-MeV ($0^+$) state[2] via a 6.52-MeV $\gamma$ ray. Observation of this $\gamma$ ray in singles and in triple coincidence yielded a positron-detection efficiency of 2.9%. However, the error in this measurement is unknown as the error in the 12% decay branch was not quoted in Ref. 2.

## III. RESULTS AND ANALYSIS

### A. Lifetimes

The technique used for analyzing the $(p,p'\gamma)$ lifetime data has been described previously.[20] The coincidence $\gamma$-ray spectra of Fig. 3, typical of several obtained during the experiment, indicate the observed Doppler shift of the 3.90-MeV $\gamma$ ray (double-escape peak) at forward and backward angles of observation. Both full-energy and double-escape peaks were analyzed for several individual runs; a weighted-average attenuation factor of $0.932\pm0.009$ was obtained. The quoted value of $F(\tau)$ contains a 0.5% correction for $\gamma$-ray angular-correlation effects; the error in $F(\tau)$ has equal contributions due to statistical errors in the centroid determination and error as a result of $\pm0.5°$ estimated uncertainty in detector angle. The $F(\tau)$ curve of Fig. 4 was calculated using the formalisms of Lindhard, Scharff, and Schiøtt (LSS)[21] for electronic and nuclear stopping and Blaugrund[22] for large-angle scattering. An electronic stopping power 20% larger than that predicted by LSS[21] was used in the calculation. This value was obtained by interpolation between existing experimental stopping-power data.[23-26] A value $\tau=(48\pm10)$ fsec was obtained for the mean lifetime of the 3.90-MeV ($2^+$) state of $Ca^{40}$ from the $F(\tau)$ curve of Fig. 3. The quoted error in lifetime includes the effect

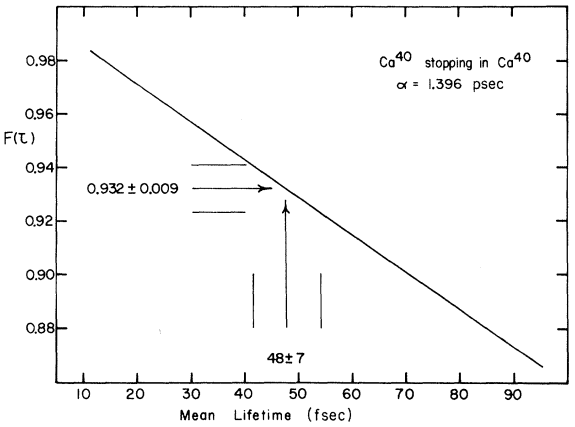


FIG. 4. Attenuation factor versus mean lifetime for $Ca^{40}$ ions with an initial velocity $v_0=5.098\times10^{-3}c$ stopping in $Ca^{40}$.

on the $F(\tau)$ curve of a possible $\pm15\%$ error in electronic- and nuclear-stopping-power values added in quadrature to the experimental errors. A similar measurement of the Doppler-shift attenuation for the 5.28-MeV ($4^+$)→ 3.90-MeV ($2^+$) transition in $Ca^{40}$ resulted in a measured $F(\tau)=0.655\pm0.025$ corresponding to a mean lifetime of $310\pm60$ fsec for the $4^+$ state. This lifetime, which includes uncertainties in stopping powers, compares favorably with other measurements[5-7] and provides a useful check on the experimental and analysis procedures.

Figure 5 shows 90 and 0° singles $\gamma$-ray spectra obtained from the $K^{39}(p,\gamma)Ca^{40}$ reaction at the $E_p$

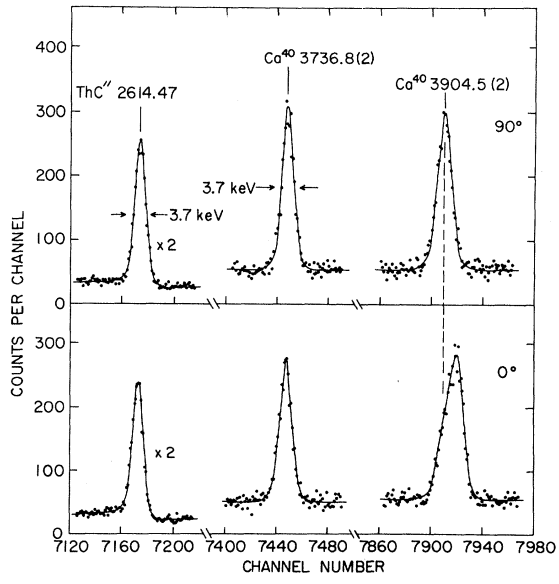


FIG. 5. $\gamma$-ray spectra from the reaction $K^{39}(p'\gamma)Ca^{40}$ obtained at 0 and 90° with respect to the incident proton beam. The "double-escape" peak of the 3.90-MeV $\gamma$ ray exhibits a Doppler shift corresponding to $F(\tau)=0.567\pm0.023$.

= 1.344-MeV resonance. As mentioned earlier, the 3.90- and 3.74-MeV $\gamma$ rays are of nearly equal intensity at this resonance. As the lifetime of the 3.74-MeV ($3^-$) state is (59 ± 5) psec,[27] its deexcitation $\gamma$ rays will not exhibit a Doppler shift and can thus be used as a reference line. The full-energy peak of the 2.614-MeV $\gamma$ rays from a ThC″ source was also included in the spectra as an additional reference. An attenuation factor $F(\tau) = 0.567 \pm 0.023$ was extracted from the 90–0° peak centroid shift. As indicated on the $F(\tau)$ curve of Fig. 6, the observed shift corresponds to a mean lifetime of (58 ± 10) fsec for the $2^+$ state. The dominant error is due to the uncertainty in the $F(\tau)$ curve. In this case, the illustrated $F(\tau)$ curve for Ca ions stopping in $K_2^{39}SO_4$ was obtained directly from theoretical estimates of stopping powers and large-angle scattering.

In addition to the centroid-shift analysis of the data, the line shape of the 3.90-MeV double-escape peak was calculated as a function of mean lifetime. Figure 7(a) indicates the best line-shape fit obtained; Fig. 7(b) shows the normalized $\chi^2$ as a function of the variable parameter $\tau$. The mean lifetime corresponding to the best fit is (58 ± 10) fsec, in excellent agreement with the centroid-shift analysis.

### B. Branching Ratio

#### 1. $(p,p'\gamma)$ Measurement

The $\gamma$-ray spectrum of Fig. 8 is the sum of the four quadruple-coincidence spectra obtained in each of the NaI(Tl) detectors. There is a prominent peak at 0.555 MeV, as well as background events which are probably due to bremsstrahlung and multiple-scattering processes. The line shape drawn through the data points indicates the detector response to 0.511-MeV radiation obtained from calibration runs with a $Na^{22}$ source. The number of counts in the 0.555-MeV photopeak is 250 ± 20 where the error is due to statistical uncertainties.

The total number of excitations of the 3.90-MeV ($2^+$) level for which a proton was detected in the surface-barrier detector was measured to be $(1.71 \pm 0.05) \times 10^8$. This number was derived by scaling the appropriate proton group and making small corrections for the tails of higher-energy

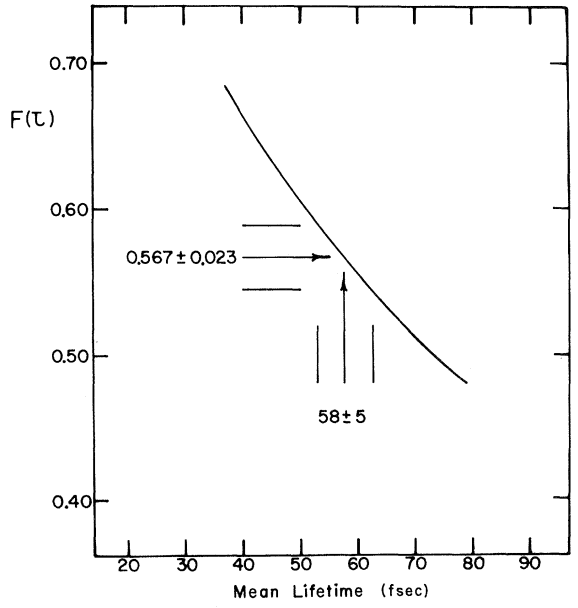


FIG. 6. $F(\tau)$ curve for $Ca^{40}$ ions stopping in $K_2^{39}SO_4$. The indicated error in $\tau$ does not include error due to uncertainties in the stopping cross sections and the subsequent uncertainty in the $F(\tau)$ curve.

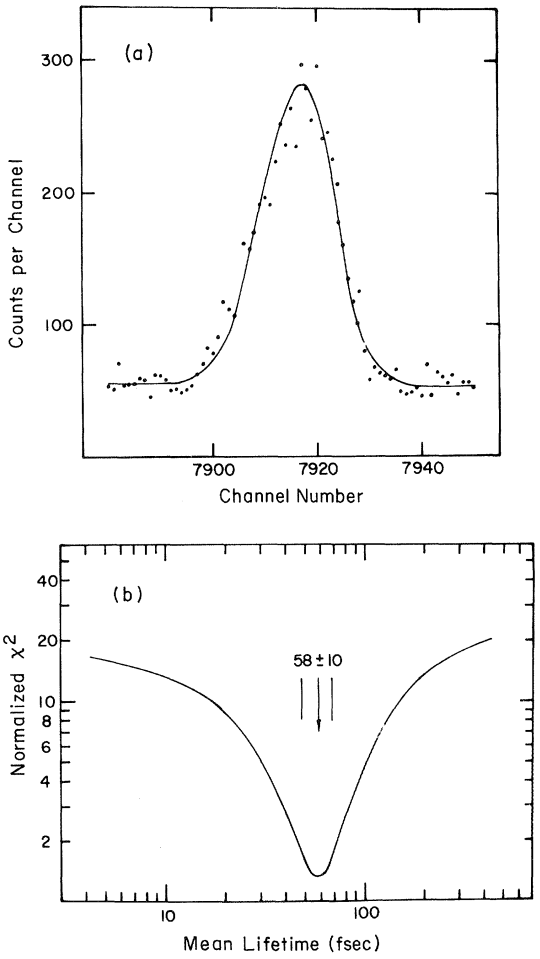


FIG. 7. (a) Line-shape fit to the "double-escape" peak of the 3.90-MeV $\gamma$ ray observed at 0°. The detector response was taken from the line shape of the unshifted 3.74-MeV $\gamma$ ray. (b) Normalized $\chi^2$ as a function of mean lifetime for the line-shape fit. A mean lifetime of 58 ±10 fsec is indicated; the error is statistical and corresponds to two standard deviations.

proton groups included in the window. The number of 0.555-MeV $\gamma$ rays in the photopeak of the spectrum of Fig. 8 is simply given by the product of the number of excitations, the efficiency for detecting positrons, the photopeak efficiency for detecting 0.555-MeV $\gamma$ rays and the cascade-to-crossover branching ratio $R$. In addition, corrections must be applied for system dead time as well as for angular-correlation effects. The angular correlation of the 0.555-MeV cascade $\gamma$ rays must be identical to that of the 3.90-MeV crossover transition. Using the latter correlation, which was measured to be $W(\theta) = 1 + 0.45P_2(\cos\theta) + 0.40P_4(\cos\theta)$, and geometrical attenuation coefficients appropriate to the detection of 0.555-MeV $\gamma$ rays, a multiplicative correlation factor of 1.13 must be applied to convert the 90° $\gamma$ yield into a total yield. The error in this correction factor is negligible. The branching ratio extracted from the data of Fig. 8 is

$$R = \frac{\text{Intensity } (3.90 \rightarrow 3.35)}{\text{Intensity } (3.90 \rightarrow 0)} = (7.73 \pm 0.93) \times 10^{-4} .$$

The quoted error includes uncertainties in detector efficiencies added in quadrature to the dominant statistical error.

### 2. $(p,\gamma)$ Measurement

Figure 9 shows the spectrum used in the analysis of the 3.90→3.35-MeV branching ratio. This spectrum is the sum of the triple-coincidence anticoincidence spectra of the four separate detectors after normalizing the peak position of the 0.511-MeV line. The data were accumulated in three separate runs for a total time of 138 h at an average beam current of 9 $\mu$A. Between runs, $Na^{22}$ singles spectra were taken for calibration purposes. The spectrum of Fig. 9 contains a residual 0.511-MeV peak not completely removed by the anticoincidence condition, a high-energy tail on this peak suggesting the presence of a 0.555-MeV line and a background continuum which results from bremsstrahlung and the Compton distribution of high-energy $\gamma$ rays. Random coincidences were negligible. The $Na^{22}$ calibration spectra for the four detectors were also normalized and summed in the same way as for the $K^{39}+p$ spectra. The shape of the 0.511-MeV line in the resulting spectrum was used in the analysis of the triple-coincidence data; the energy dispersion was derived from the separation of the 0.511- and 1.275-MeV peaks. Using this dispersion, together with an energy of 0.555 MeV for the 3.90→3.35-MeV transition as measured by Canada *et al.*,[19] the position of the 0.555-MeV peak was calculated to be 12.7 channels higher than the 0.511-MeV line as indicated in Fig. 9. The complete spectrum was then assumed to consist of two peaks at channels 161 and 173.7 having the shape of the 0.511-MeV instrumental line discussed above, superimposed on a background. The background was considered to be a constant plus an exponential component, and a best fit was first obtained for the background spectrum between channels 110 and 143 and between channels 188 and 240. In the final fitting of the total spectrum the amplitudes of the two peaks were the only free parameters. The computer fit showed that the intensities of the 0.511- and 0.555-MeV peaks in Fig. 9 were 7031 ± 167 and 1081 ± 134 counts, respectively. The $\chi^2$ for the fit was 1.34.

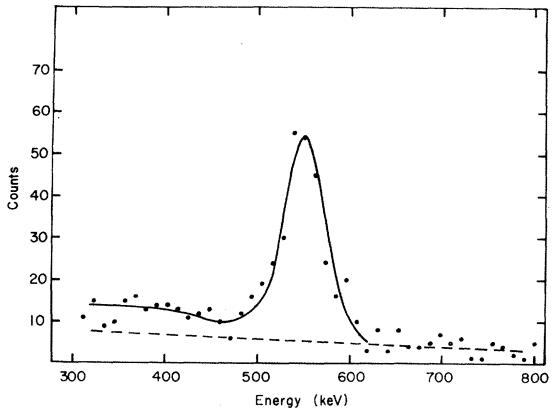


FIG. 8. $\gamma$ rays in quadruple coincidence with inelastically scattered protons populating the 3.90-MeV ($2^+$) level of $Ca^{40}$ and two annihilation quanta from the pair decay of the 3.35-MeV ($0^+$) state. The line drawn through the photopeak of the 0.555-MeV cascade $\gamma$ ray is derived from the detector response to 0.511-MeV radiation.

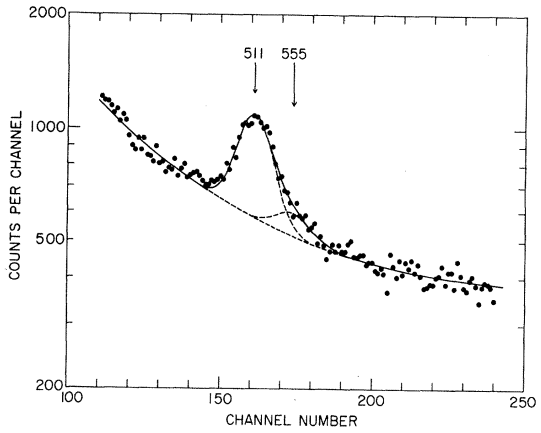


FIG. 9. Spectrum of $\gamma$ rays in triple coincidence with annihilation radiation from the reaction $K^{39}(p,\gamma)Ca^{40}$ at the $E_p = 1.344$-MeV resonance. The curves are a least-squares fit to the data and indicate 0.511- and 0.555-MeV photopeaks as well as constant-plus-exponential background.

In order to check the consistency of the results the four individual spectra were analyzed in the same way as for the sum spectrum, i.e., the summed $Na^{22}$ 0.511-MeV peak for each detector was used as the calibration line shape for analyzing the $K^{39}+p$ spectrum of that detector. Although the separate analyses all gave positive indications for the presence of the 0.555-MeV peak the values of the ratio $I_{0.555}/I_{0.511}$ from the separate computer fits did not all overlap within the statistical accuracies of the individual fits. It was further noted that there were unexplained differences in the shapes of the backgrounds of the separate spectra. It was concluded that the curve-fitting procedure was not as accurate as indicated by the computer fit and that to obtain satisfactory consistency the errors given by the computer fit should be doubled. We therefore state that the intensity of the unresolved 0.555-MeV line in Fig. 9 is $1081 \pm 270$ counts.

The total number of 3.90-MeV transitions for the entire run was calculated from analyses of several of the singles spectra from the 5-in. $\times$ 5-in. NaI(Tl) monitor detector. These spectra contained the partially resolved 3.74- and 3.90-MeV full-energy-loss peaks. From the total area under the combined 3.74 + 3.90 photopeaks and the known intensity ratio of these $\gamma$ rays quoted earlier, the net area under the 3.90-MeV photopeak was found. This was corrected for the absolute photopeak efficiency, analyzer dead time, and $\gamma$-ray absorption in the wall of the target chamber to find the number of 3.90-MeV $\gamma$ rays emitted for a given number of counts in a scaler that recorded all $\gamma$ rays above 3 MeV. The total scaler count for the entire run was then used to find the total emission of 3.90-MeV $\gamma$ rays corresponding to the coincidence data of Fig. 9.

The $3.90 \rightarrow 3.35$-MeV $\gamma$-ray branching ratio was calculated from the number of counts in the 0.555-MeV peak knowing the number of 3.90-MeV states populated, the positron-detection efficiency, the 0.555-MeV photopeak efficiency, and the $\gamma$-ray absorption. The positron-detection efficiency took into account a 7% loss of coincidences due to those positrons which emerged at approximately 180° to the beam direction and did not annihilate between the crystals. In addition, a correction was made for summing wherein the 5.74-MeV $\gamma$ ray feeding the 3.90-MeV state interacted in one of the crystals. This effect resulted in a 13.6% loss of counts in the 0.555-MeV triple-coincidence peak. The $3.90 \rightarrow 3.35$-MeV branch determined from this analysis of the $K^{39}(p,\gamma)Ca^{40}$ experiment is $(7.2 \pm 2.6) \times 10^{-4}$.

## IV. DISCUSSION

The lifetime of the 3.90-MeV level extracted from the $(p,p'\gamma)$ data is in good agreement with that obtained previously using a similar technique[5] (Table I). Furthermore, the result agrees well with the work of Start *et al.*,[13] who used the $(p,p'\gamma)$ reaction at different bombarding energies and at different particle-detection angles in order to vary the nuclear recoil energy and hence change the $F(\tau)$ curve. The result is also consistent with the resonance-fluorescence measurement of Rasmussen[17] and the inelastic electron scattering results of Eisenstein *et al.*[15]

The present $(p,\gamma)$ result, although consistent with the above-mentioned work, is totally inconsistent with the previous $(p,\gamma)$ data of Lindeman *et al.*[8] and Dolan and McDaniels.[7] The disagreement is in the measured Doppler shift and not in the $F(\tau)$ curve used to extract the lifetime from the observed shift. In view of the obvious inconsistency in the $(p,\gamma)$ lifetime data of Table I, we adopt a weighted average of $(50 \pm 5)$ fsec for the mean lifetime of the 3.90-MeV $(2^+)$ state, which does not include the earlier $(p,\gamma)$ or electron scattering results. Table II summarizes available data on the lifetime of the 5.28-MeV $(4^+)$ state; a value of $(310 \pm 60)$ fsec is adopted for the mean lifetime of this state.

The branching ratio $R = (7.7 \pm 0.9) \times 10^{-4}$ extracted from the present $(p,p'\gamma)$ data is in good agreement with the value $R = (8.7 \pm 1.4) \times 10^{-4}$ obtained by Cana-

TABLE II. Summary of measurements of the mean lifetime of the 5.28-MeV $(4^+)$ state of $Ca^{40}$.

| Experimental technique | Mean lifetime (fsec) |
|---|---|
| Doppler-shift attenuation, $K^{39}(p,\gamma)Ca^{40}$ [a] | $\geq 190$ |
| Doppler-shift attenuation, $K^{39}(p,\gamma)Ca^{40}$ [b] | $230^{+190}_{-60}$ |
| Doppler-shift attenuation, $Ca^{40}(p,p'\gamma)Ca^{40}$ [c] | $410 \pm 100$ |
| Doppler-shift attenuation, $Ca^{40}(p,p'\gamma)Ca^{40}$ [d] | $260 \pm 80$ |
| Doppler-shift attenuation, $Ca^{40}(p,p'\gamma)Ca^{40}$ [e] | $310 \pm 60$ |
| Adopted value | $310 \pm 60$ |

[a] See Ref. 8.
[b] See Ref. 7.
[c] See Ref. 6.
[d] See Ref. 5.
[e] Present work.

da *et al.*[19] These workers excited the 3.90-MeV state via the $(p,p')$ reaction at a bombarding energy of 6.14 MeV and detected the 0.555-MeV decay $\gamma$ rays in a Ge(Li) counter in coincidence with two annihilation quanta recorded in large NaI(Tl) detectors. The value $R=(7.2\pm2.6)\times10^{-4}$ obtained in the present $(p,\gamma)$ experiment is quite consistent with the above measurements, and we adopt an over-all average $R=(7.95\pm0.8)\times10^{-4}$ with the measurements weighted inversely as the square of the absolute error.

We note that this branching ratio is larger than the limit $R<3\times10^{-4}$ found in a less refined preliminary experiment.[18] The difficulty in reconciling the $(p,\gamma)$ triple-coincidence count rates of the present experiment in the four different combinations of detectors indicates that the errors previously assigned may have been underestimated. Doubling the errors as generated by the fitting procedure in the preliminary experiment lessens, but does not remove, the discrepancy. The observed situation, wherein three $(p,\gamma)$ measurements of the decay properties of the $2^+$ state give results seemingly inconsistent with other experiments, cannot be considered to be entirely satisfactory.

The positions and decay properties of most of the positive-parity levels in $Ca^{40}$ are adequately accounted for by the theoretical description of Gerace and Green.[11,12] These authors describe the states in terms of wave functions obtained by promoting even numbers of particles from the $2s$-$1d$ shell into the $2p$-$1f$ shell. The majority components of deformed-state wave functions are shown in Table III, both for axially symmetric $K=0$ prolate states and for $K=2$ axially asymmetric states. The predicted transition strengths indicated in the table are generally smaller than, but in fair agreement with the experimental strengths. Predicted in-band transition strengths are largely due to the predominant components of the wave functions listed in the table while interband transitions involve minority components (including $K$ mixing). As the latter transitions in many cases involve matrix-element cancellations of minority components, only qualitative agreement is expected (and indeed found). The model successfully reproduces the observed in-band $B(E2;$ 3.90 MeV $(2^+)\rightarrow$ 3.35 MeV $(0^+))$, but underestimates the crossover transition strength by a factor of roughly 3. However, a small increase in the amplitude of the 4p-4h deformed-state component in the predominantly 0p-0h ground-state wave function would bring pre-

TABLE III. Experimental and theoretical $B(E2)$ values in $Ca^{40}$. These levels are characterized according to the scheme of Ref. 12.

| Transition From | | | Transition To | | | $B(E2)$ ($e^2$fm$^4$) | | |
|---|---|---|---|---|---|---|---|---|
| Level (MeV) | | Character | Level (MeV) | | Character | Experimental [a] | Theoretical Deformed [b] | Theoretical Spherical [c] |
| 3.90 | $2^+$ | ($K=0$, 4p-4h) | 0 | $0^+$ | ($K=0$, 0p-0h) | $18\pm1.8$ | 6 | 17 |
| | | | 3.35 | $0^+$ | ($K=0$, 4p-4h) | $250\pm35$ | 253 | 188 |
| 5.28 | $4^+$ | ($K=0$, 4p-4h) | 3.90 | $2^+$ | ($K=0$, 4p-4h) | $535\pm110$ | 370 | |
| 5.25 | $2^+$ | ($K=2$, 4p-4h) | 0 | $0^+$ | ($K=0$, 0p-0h) | $0.8\pm0.1$ | 0 | 3.7 |
| | | | 3.35 | $0^+$ | ($K=0$, 4p-4h) | $6.5\pm3.3$ | 7.5 | 3.4 |
| | | | 3.90 | $2^+$ | ($K=0$, 4p-4h) | $140\pm40$ | 124 | 94.7 |
| 6.03 | $3^+$ | ($K=2$, 4p-4h) | 3.90 | $2^+$ | ($K=0$, 4p-4h) | $32\pm8$ | 10 | |
| | | | 5.25 | $2^+$ | ($K=2$, 4p-4h) | $730\pm300$ | 440 | |
| | | | 5.28 | $4^+$ | ($K=0$, 4p-4h) | $<180$ | | |
| 6.51 | $4^+$ | ($K=2$, 4p-4h) | 3.90 | $2^+$ | ($K=0$, 4p-4h) | $35^{+20}_{-11}$ | 3.9 | |
| | | | 5.25 | $2^+$ | ($K=2$, 4p-4h) | $200^{+150}_{-75}$ | 115 | |
| | | | 5.28 | $4^+$ | ($K=0$, 4p-4h) | $52\pm44$ | 64 | |
| | | | 5.63 | $2^+$ | ($K=0$, 8p-8h) | $<480$ | | |
| 5.21 | $0^+$ | ($K=0$, 8p-8h) | 3.90 | $2^+$ | ($K=0$, 4p-4h) | $110\pm20$ | 26 | 41.6 |
| 5.63 | $2^+$ | ($K=0$, 8p-8h) | 0 | $0^+$ | ($K=0$, 0p-0h) | $1.6\pm0.5$ | 1.5 | 0 |
| | | | 3.35 | $0^+$ | ($K=0$, 4p-4h) | $22\pm11$ | 26 | 12.1 |
| | | | 3.90 | $2^+$ | ($K=0$, 4p-4h) | $<21$ | 12.5 | 3.2 |
| 6.54 | $(4^+)$ | ($K=0$, 8p-8h) | 3.90 | $2^+$ | ($K=0$, 4p-4h) | $24^{+11}_{-7}$ | 18 | |
| | | | 5.25 | $2^+$ | ($K=2$, 4p-4h) | $105\pm50$ | | |
| | | | 5.28 | $4^+$ | ($K=0$, 4p-4h) | $\leq92\pm50$ [d] | 16 | |
| | | | 5.63 | $2^+$ | ($K=0$, 8p-8h) | $820^{+450}_{-280}$ | 720 | |
| 6.91 | $2^+$ | ($K=0$, 2p-2h) | 0 | $0^+$ | ($K=0$, 0p-0h) | $14\pm4$ | 6 | 3.8 |

[a] See Refs. 1–10, 15, 19 and the present work.
[b] See Ref. 12.
[c] See Ref. 28.
[d] The $E2/M1$ mixing ratio is not known for this transition. The quoted $B(E2)$ value assumes a pure $E2$ transition.

dicted and observed strengths into agreement.

An alternate approach to the nuclear structure of $0^+$ and $2^+$ states has been made by Federman and Pittel.[28] These authors consider spherical 0p-0h, 2p-2h, and 4p-4h states, restricting the orbitals to $1f_{7/2}$ and $1d_{3/2}$ for particles and holes, respectively. The basis was further truncated by the elimination of the more highly excited basis states. The calculated positions of $0^+$ and $2^+$ states are in reasonable agreement with the experimental spectrum. Transition probabilities were calculated using harmonic-oscillator wave functions (an oscillator energy of 10.5 MeV) and a total effective charge $e_n + e_p = 2.9$. The results are compared with experiment in Table III with fair agreement evident although strong transitions (which, in the deformed-state description, are due to collective behavior) are underestimated. Furthermore, the effective charge used in the calculation is rather high. Use of an effective charge $e_n + e_p = 2$, which seems appropriate in the case of transitions between negative-parity states,[29] further reduces the calculated strengths by a factor of 2.

It is not possible to distinguish between a deformed basis and a sufficiently extended spherical basis, but it is evident both that the truncation of the present spherical-basis calculations has been made too soon and that sufficiently extended calculations on an adequate spherical basis are not a practical proposition. This is not to say that microscopic calculations on a spherical basis are not valuable in giving a feeling for the way in which collectivity begins to arise but rather that calculations on a deformed basis probably give a more nearly literal picture of the actual situation.

## ACKNOWLEDGMENTS

The authors acknowledge helpful discussions with Dr. M. A. Grace, Dr. R. Anderson, and Dr. D. F. H. Start. We thank Dr. N. Benczer-Koller, Dr. R. D. Gill, H. P. Lie, J. Tape, Lewis Guthman, and R. Hensler for their assistance in some parts of the work. We thank Professor A. M. Green for an informative correspondence. G. Sullivan Read, Jr., assisted in the analysis of some of the data.

---

†Research at Brookhaven National Laboratory carried out under the auspices of the U. S. Atomic Energy Commission.

[1]M. A. Grace and A. R. Poletti, Nucl. Phys. 78, 273 (1966).

[2]H. P. Leenhouts and P. M. Endt, Physica 32, 322 (1966).

[3]H. P. Leenhouts, Physica 35, 290 (1967).

[4]R. W. Bauer, A. M. Bernstein, G. Heymann, E. P. Lippincott, and N. S. Wall, Phys. Letters 14, 129 (1965).

[5]Jack R. MacDonald, D. F. H. Start, R. Anderson, A. G. Robertson, and M. A. Grace, Nucl. Phys. A108, 6 (1968).

[6]A. R. Poletti, A. D. W. Jones, J. A. Becker, and R. E. McDonald, Phys. Rev. 181, 1606 (1969).

[7]K. W. Dolan and D. K. McDaniels, Phys. Rev. 175, 1446 (1968).

[8]H. Lindeman, G. A. P. Engelbertink, M. W. Ockeleon, and H. S. Pruys, Nucl. Phys. A122, 373 (1968).

[9]R. Anderson, A. G. Robertson, D. F. H. Start, L. E. Carlson, and M. A. Grace, Nucl. Phys. A131, 113 (1969).

[10]F. R. Metzger, Phys. Rev. 165, 1245 (1968).

[11]W. J. Gerace and A. M. Green, Nucl. Phys. 93, 110 (1967).

[12]W. J. Gerace and A. M. Green, Nucl. Phys. A123, 241 (1969).

[13]D. F. H. Start, private communication.

[14]D. Blum, P. Barreau, and J. Bellicard, Phys. Letters 4, 109 (1963).

[15]R. A. Eisenstein, D. W. Madsen, H. Theissen, L. S. Cardman, and C. K. Bockelman, Phys. Rev. 188, 1815 (1969).

[16]E. C. Booth and K. A. Wright, Nucl. Phys. 35, 472 (1962).

[17]V. K. Rasmussen, private communication.

[18]Jack R. MacDonald, D. H. Wilkinson, and D. E. Alburger, Bull. Am. Phys. Soc. 13, 695 (1968).

[19]T. R. Canada, R. S. Cox, J. S. Duval, C. H. Sinex, and C. M. Class, Phys. Rev. 188, 1741 (1969).

[20]M. C. Bertin, N. Benczer-Koller, G. C. Seaman, and Jack R. MacDonald, Phys. Rev. 183, 964 (1969).

[21]J. Lindhard, M. Scharff, and H. Schiøtt, Kgl. Danske Videnskab. Selskab, Mat.-Fys. Medd. 33, No. 14 (1963).

[22]A. E. Blaugrund, Nucl. Phys. 88, 501 (1966).

[23]L. C. Northcliffe, Ann. Rev. Nucl. Sci. 13, 67 (1963).

[24]D. I. Porat and K. Ramavataran, Proc. Phys. Soc. (London) 77, 97 (1960); 78, 1135 (1961).

[25]J. H. Ormrod and H. E. Duckworth, Can. J. Phys. 41, 1424 (1963).

[26]J. H. Ormrod, J. R. MacDonald, and H. E. Duckworth, Can. J. Phys. 43, 275 (1965).

[27]J. Tape, N. Benczer-Koller, R. Hensler, L. Guthman, and Jack R. MacDonald, private communication.

[28]P. Federman and S. Pittel, Phys. Rev. 186, 1106 (1969); Nucl. Phys. 139, 108 (1969).

[29]Jack R. MacDonald, N. Benczer-Koller, J. Tape, L. Guthman, and P. Goode, Phys. Rev. Letters 23, 594 (1969).